the plant journal

SEB SOCIETY FOR EXPERIMENTAL BIOLOGY

The Plant Journal (2024) **117,** 909–923 doi: 10.1111/tpj.16537

A DELAY OF GERMINATION 1 (DOG1)-like protein regulates spore germination in the moss *Physcomitrium patens*

Evelyn Vollmeister[1], Alexandros Phokas[2,†], Rabea Meyberg[1], Clemens V. Böhm[1], Marlies Peter[1], Eva Kohnert[3], Jinhong Yuan[4], Christopher Grosche[1], Marco Göttig[1], Kristian K. Ullrich[1,‡], Pierre-François Perroud[1,§], Andreas Hiltbrunner[4,5], Clemens Kreutz[3], Juliet C. Coates[2] and Stefan A. Rensing[1,6,*,¶]

[1]*Plant Cell Biology, Department of Biology, University of Marburg, Marburg, Germany,*
[2]*School of Biosciences, University of Birmingham, Edgbaston, Birmingham B15 2TT, UK,*
[3]*Institute of Medical Biometry and Statistics, Medical Center, Faculty of Medicine, University of Freiburg, Freiburg 79104, Germany,*
[4]*Faculty of Biology, University of Freiburg, Freiburg, Germany,*
[5]*Signalling Research Centres BIOSS and CIBSS, University of Freiburg, Germany,*
[6]*BIOSS Centre for Biological Signalling Studies, University of Freiburg, Freiburg, Germany*

Received 12 November 2022; revised 22 October 2023; accepted 26 October 2023; published online 13 November 2023.
*For correspondence (e-mail stefan.rensing@cup.uni-freiburg.de).
[†]Present address: Department of Agrobiotechnology, Agricultural Research Institute, Nicosia, Cyprus
[‡]Present address: Department of Evolutionary Genetics, Max Planck Institute for Evolutionary Biology, Plön, Germany
[§]Present address: Université Paris-Saclay, INRAE, AgroParisTech, Institut Jean-Pierre Bourgin (IJPB), Versailles 78000, France
[¶]Present address: Faculty of Chemistry and Pharmacy, University of Freiburg, Freiburg, Germany

SUMMARY

DELAY OF GERMINATION 1 is a key regulator of dormancy in flowering plants before seed germination. Bryophytes develop haploid spores with an analogous function to seeds. Here, we investigate whether DOG1 function during germination is conserved between bryophytes and flowering plants and analyse the underlying mechanism of DOG1 action in the moss *Physcomitrium patens*. Phylogenetic and *in silico* expression analyses were performed to identify and characterise DOG1 domain-containing genes in *P. patens*. Germination assays were performed to characterise a *Ppdog1-like1* mutant, and replacement with *At*DOG1 was carried out. Yeast two-hybrid assays were used to test the interaction of the *Pp*DOG1-like protein with DELLA proteins from *P. patens* and *A. thaliana*. *P. patens* possesses nine DOG1 domain-containing genes. The DOG1-like protein *Pp*DOG1-L1 (*Pp*3c3_9650) interacts with *Pp*DELLAa and *Pp*DELLAb and the *A. thaliana* DELLA protein *At*RGA in yeast. Protein truncations revealed the DOG1 domain as necessary and sufficient for interaction with *Pp*DELLA proteins. Spores of *Ppdog1-l1* mutant germinate faster than wild type, but replacement with *At*DOG1 reverses this effect. Our data demonstrate a role for the *Pp*DOG1-LIKE1 protein in moss spore germination, possibly alongside *Pp*DELLAs. This suggests a conserved DOG1 domain function in germination, albeit with differential adaptation of regulatory networks in seed and spore germination.

Keywords: DELAY OF GERMINATION 1, DELLA, DOG1, dormancy, evolution, *Physcomitrium patens*, spore germination.

INTRODUCTION

The timing of germination is a crucial step in the life cycle of a plant, determining the survival of the subsequent generation and thus reproductive success (Graeber et al., 2014; Merai et al., 2019; Moody et al., 2016). In Spermatophyta (seed plants), the structure that germinates to start a new plant generation is the multicellular diploid seed. The ability of a seed to germinate depends on two physically opposite forces, embryo growth and limitation by tissue layers (Finch-Savage & Leubner-Metzger, 2006). Under favourable environmental conditions (Huo et al., 2016), germination proceeds as follows: after imbibition (intake of water) and potential mucilage formation, a combination of hydrolytic enzymes of the endosperm and mechanical pressure of the growing embryo cause the hard seed coat to break open with the appearance of the radicle as an external sign of germination (Graeber et al., 2014; Holdsworth et al., 2008). Before a seed germinates, it proceeds through a temporary

resting state. During this phase, developmental processes such as seed maturation and after-ripening take place (Holdsworth et al., 2008). Dormancy is induced during seed maturation and is important for surviving adverse environmental conditions and taking advantage of the optimal conditions of seasons and particular habitats and can last multiple years (Gremer et al., 2016).

The moss *Physcomitrium patens*, a model organism for non-seed plants, is part of the bryophytes that are sister to seed plants (Puttick et al., 2018; Rensing et al., 2020). The *P. patens* life cycle begins with the germination of an imbibed unicellular haploid spore (Vesty et al., 2016). Filamentous protonemata begin to grow and spread through two-dimensional tip growth and branching (Menand et al., 2007). Subsequently, a switch to three-dimensional growth occurs and multicellular leafy gametophores develop (Harrison et al., 2009). In autumn, sexual reproductive tissues (gametangia) develop at the tip of the gametophore (Hiss, Meyberg, et al., 2017). After fertilisation, the development of diploid sporophytes takes place. Embryogenesis occurs within the archegonium, which later ruptures and becomes the calyptra. The spore mother cells develop inside of the now bulb-shaped young sporophyte, and after meiosis, the haploid spores of the new generation mature. The dried sporophyte ruptures and the spores are dispersed (Rensing et al., 2020).

In seed plants, the initiation and maintenance of the dormancy phase is controlled by the hormones gibberellic acid (GA) and abscisic acid (ABA) and is regulated by the interplay of their signalling pathways (Carrera-Castano et al., 2020; Holdsworth et al., 2008; Liu & Hou, 2018; Shu et al., 2018). In the seed plant GA signalling pathway, DELLA proteins are positive regulators of dormancy by acting as inhibitors of the transcription of GA target genes (Yoshida et al., 2014). In the presence of GA, GID1 (GIBBERELLIN INSENSITIVE DWARF 1) promotes the interaction of DELLA with the SKP1-CULLIN-F-BOX/SLEEPY1 (SCF/SLY1) protein complex (Hirano et al., 2010; Murase et al., 2008; Ueguchi-Tanaka et al., 2005). Subsequent polyubiquitination of DELLA leads to its degradation through the 26S proteasome pathway (Fu et al., 2002; Sasaki et al., 2003), whereby germination is promoted (Rombola-Caldentey et al., 2014). In *Arabidopsis thaliana*, five DELLA proteins were identified: GA-INSENSITIVE, GAI; REPRESSOR OF GAI 1, RGA; RGA-LIKE1, RGL1; RGL2; RGL3 (Daviere & Achard, 2013). RGL2 is primarily responsible for inhibiting seed germination (Lee et al., 2002), while the other proteins perform functions such as inhibiting GA-dependent floral initiation or suppressing flower development as well as acting as a transcriptional activator (Cheng et al., 2004; King et al., 2001; Tyler et al., 2004).

With regard to GA-based regulation of germination in seed plants, DELAY OF GERMINATION 1 (DOG1) was identified as a quantitative trait locus controlling seed dormancy in *A. thaliana* (Bentsink et al., 2006). DOG1 acts by inhibiting the expression of GA-regulated genes to promote dormancy (Graeber et al., 2014). Although DOG1 functions independently of ABA (Nakabayashi et al., 2012), regulation of dormancy by DOG1 requires a functional ABA signalling pathway (Kendall et al., 2011; Nakabayashi et al., 2012). DOG1 controls dormancy by repressing specific PROTEIN PHOSPHATASE 2C (PP2C) phosphatases that act as points of convergence between ABA signalling pathways and DOG1 signalling pathways (Nee et al., 2017; Nishimura et al., 2018).

The number of DOG1 domain-containing proteins varies among plant species. Their function is important for seed germination and related functions, such as seed degreening or induction of desiccation tolerance (Dekkers et al., 2016; Sall et al., 2019). However, during evolution, the function of DOG1 and related proteins has diversified phylogenetically, for example, for *TGACG motif-binding transcription factor* (TGAs) and DOG1-like proteins (Nishiyama et al., 2021; Sall et al., 2019). In *A. thaliana*, there is one DOG1 and five DOG-like (DOGL; DOGL1-5) proteins (Nishiyama et al., 2021). *At*DOG1, (*A. thaliana*, AT5G45830.1) is characterised by the presence of the DOG1 protein domain (Bentsink et al., 2006). DOG1 domains belong to a family with five distinct clades. Clade 1–4 proteins show structural similarities to *At*DOG1. Clade five proteins harbour additional DNA-interacting domains, for example, bZIP (basic leucine zipper) domains, suggesting a direct effect on transcriptional activity (Ashikawa et al., 2013). DOG1 domains contain glutamine-rich regions and acidic amino acids suggesting transcriptional activation functions (Prosite: PDOC51806). However, the exact mechanism of DOG1 domain function remains to be elucidated.

To date, relatively little is known about spore dormancy and germination in bryophytes compared to knowledge of seed germination (Glime, 2017; Vesty et al., 2016). In *P. patens*, the presence of proteins containing the DOG1 domain has been shown for four TGA transcription factor like genes that belong to the bZIP family and are distinct from DOG-like genes (Nishiyama et al., 2021). Since they are part of gametophytic generation, spores are usually not considered homologous to seeds, which are sporophytic in origin (Rensing, 2016; Vesty et al., 2016). Yet, orthologs often fulfil the same function in the two alternating generations, and hence the question arises of whether the functions of relevant proteins are conserved between bryophytes and flowering plants, in other words, whether the functionality has been transferred from the gametophyte to the sporophyte (Kenrick, 2017). Spore germination is reduced by ABA in *P. patens* (Moody et al., 2016; Vesty et al., 2016), but non-seed plants lack a complete GA biosynthesis pathway and do not synthesise gibberellins: the gibberellin precursor *ent*-kaurenoic acid (KA) is present and a metabolite of KA, 3-OH-KA, functions as the

endogenous bioactive diterpenoid in *P. patens* (Miyazaki et al., 2018). *P. patens* mutants that lack all diterpenoids show reduced spore germination (Vesty et al., 2016). Moreover, *Pp*DELLA proteins regulate spore germination, but this is independent of diterpenes (Phokas et al., 2023). Thus, the role and regulation of DOG1 and DELLA proteins in *P. patens* may be distinct from their role in seed plants. Here, we investigate the function of DOG1-like proteins in *P. patens* with respect to germination and elucidate whether the function is conserved between bryophytes and vascular plants. Furthermore, we determine which interaction partners might play a role in exerting the function of DOG1-like proteins in *P. patens*.

RESULTS

DOG1 proteins of non-seed plants harbour ankyrin (ANK) domains

DOG1-like genes are known regulators of seed germination. To investigate their function as putative regulators of plant spore germination, we screened for DOG1-domain containing homologues in the V3 genome of *P. patens* (Lang et al., 2018). In total, nine *DOG1* domain-containing genes could be identified building on previous data. Four of these genes belong to the TGA-R genes (Nishiyama et al., 2021). A further two genes, namely *Pp*3c7_19640 and *Pp*3c11_3190, contain only the DOG1 domain at the N-terminal region of the expressed protein (Figure 1a). The three remaining genes, *Pp*3c26_14620, *Pp*3c13_11750 and *Pp*3c3_9650, contain ANK repeat domains, which are known for protein–protein interactions (Sedgwick & Smerdon, 1999), in addition to DOG1 domains in the N-terminal region. Interestingly, there is an alternatively spliced, shorter form of *Pp*3c26_14620 that contains only the DOG1 domain (Figure S1). Domain structure comparison between different plant families showed that *DOG1* genes in seed plants contain only the DOG1 domain, whereas in ferns, club mosses and bryophytes some *DOG1* genes harbour additional ANK repeat domains (Figure 1a). Although ANK domain proteins exist in vascular plants such as Arabidopsis [105 ANK domain proteins in *A. thaliana* (Becerra et al., 2004)], the seed plant DOG1-like proteins appear to have lost these domains. Alternatively, non-seed plants might have gained them. In the DOG1-like proteins of bryophytes and ferns, ANK repeat domains with 2, 4 and 5 copies were found. An alignment of the DOG1 domains of *A. thaliana* and *P. patens* DOG1-like proteins demonstrates that several amino acids of *P. patens* DOG1 domains are identical to the DOG1 domain of AT5G45830.1 (Figure 1b). In particular, the C-terminal part of the domain shows a high percentage of identity.

*Pp*3c3_9650 and *Pp*3c26_14620 are expressed in sporophytes and spores

In *A. thaliana*, Bentsink and colleagues showed that *AtDOG1* is expressed in seeds (Bentsink et al., 2006). If spore germination, analogous to seed germination, is controlled by *Pp*DOG1-like proteins, one would expect stronger expression of *PpDOG1*-like genes in the spore developmental stage. To investigate whether any of the five *PpDOG1-like* genes show enriched spore expression, we used the expression atlas database PEATmoss, which contains expression data from both Gransden (Gd) and Reute (Re) ecotypes (Fernandez-Pozo et al., 2020). All five genes showed different expression patterns across different tissue types and developmental stages (Figure 2; Figure S2). The gene *Pp*3c7_19640 was found to be uniformly expressed in both Gd and Re at different developmental stages. *Pp*3c11_3190 is expressed primarily in adult gametophores (Re) and also in dry spores (Gd) but showed very low expression in imbibed and germinating spores. *Pp*3c13_11750 showed similar expression across tissue types and ecotypes. In the case of *Pp*3c26_14620, expression was highest in gametophores (Gd and Re) but also expressed in green sporophytes (Re), which contain the immature spores that later mature and turn brown. The strongest expression of any *PpDOG1*-like gene in any tissue type was found for *Pp*3c3_9650, which was most strongly expressed in spores (dry and imbibed). As spores are the functional equivalent of seeds (dispersal units) in bryophytes, and since one of the non-seed plant-unique *DOG1*-like genes with ANK domains (*Pp*3c3_9650) showed strong enrichment in spores in this analysis, we generated a knockout mutant of the *Pp*3c3_9650 gene (for the rest of the paper annotated as *PpDOG1-like 1*, *PpDOG1-L1*).

*PpDOG1-L1*knockout does not result in significant developmental differences

The knockout strain *Ppdog1-l1* was generated by homologous recombination and successfully verified via PCR and transcriptional analyses (Figure 3a,b,d). In addition, plants heterologously expressing *AtDOG1* in *Ppdog1-l1* were generated by 'knock-in' homologous recombination of a construct harbouring *AtDOG1* into the *PpDOG1-L1* locus (*Ppdog1-l1*:*AtDOG1*). Because of the restricted expression of *PpDOG1-L1*, reproductive development was compared between wild type, *Ppdog1-l1* and *Ppdog1-L1*:*AtDOG1*. Gametangia developed without obvious morphological differences and for all genotypes, immature, mature and fertilised gametangia could be observed 21 days after induction (Figure S3). *Ppdog1-l1*apices showed more and further developed archegonia (80% vs. 57% mature archegonia, not significant) and sporophytes (not significant, Figure S3) compared to wild type. Reproductive fertility was retained and spores of wild type, *Ppdog1-l1* and *Ppdog1-l1*:*AtDOG1* showed germination (Figure 3c). qPCR demonstrated that the *PpDOG1-L1* transcript is expressed in WT gametophores, but neither in the *Ppdog1-l1* mutant nor in *Ppdog1-l1*:*AtDOG1* (Figure 3d).

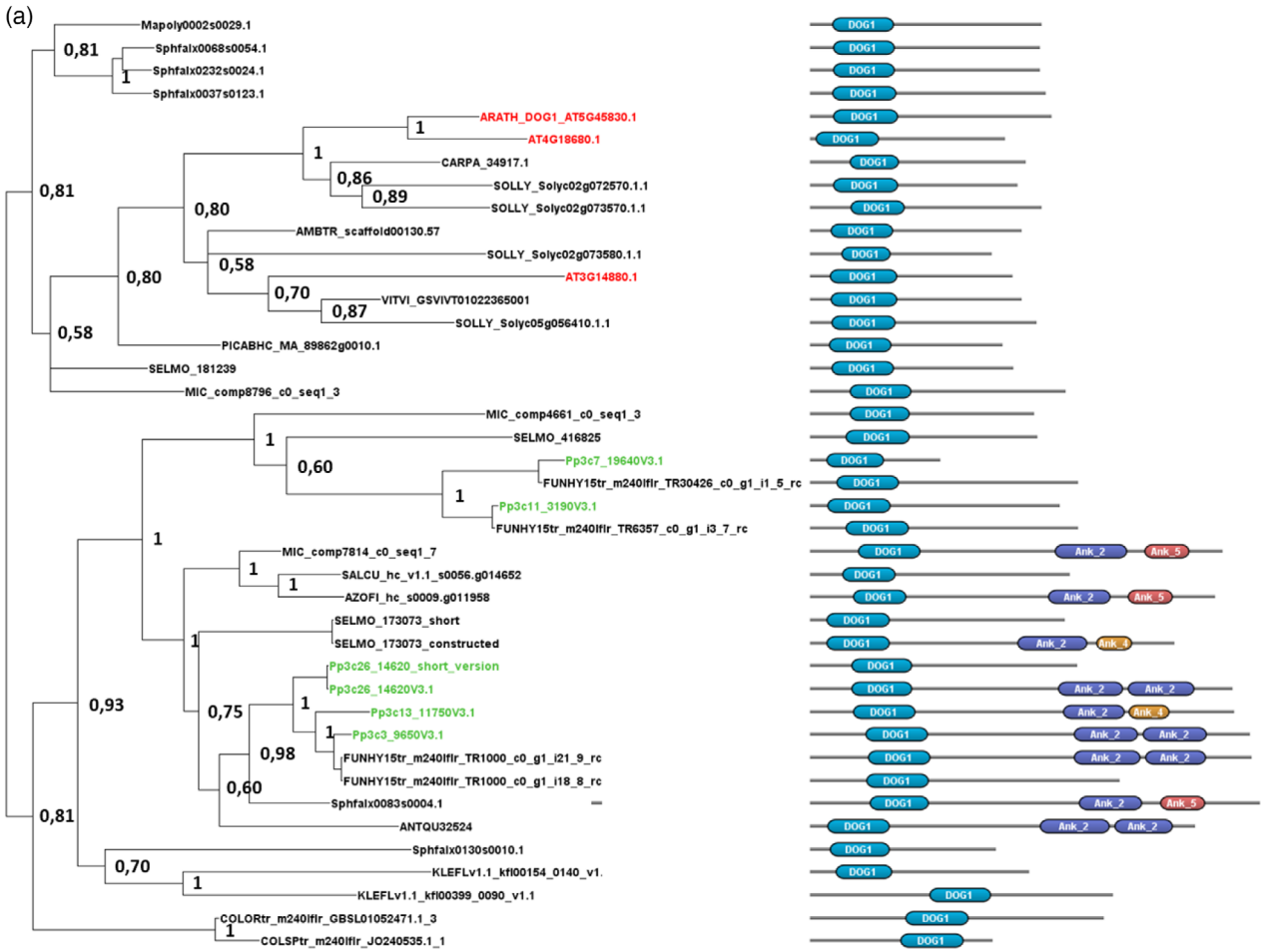

Figure 1. *In silico* analyses of DOG1 domain-containing proteins in the non-vascular plant *Physcomitrium patens*. (a) Bayesian inference phylogenetic tree of DOG1 homologues (rooted between seed-plants and non-seed plants/algae; support values at the nodes represent posterior probabilities) and their protein domain structure. Left panel: reconstruction was done using Bayesian inference. Letter codes are used to abbreviate species names (Mapoly—*Marchantia polymorpha*, Sphfalx—*Sphagnum fallax*, ARATH—*Arabidopsis thaliana*, CARPA—*Carica papaya*, SOLLY—*Solanum lycopersicum*, AMBTR—*Amborella trichpoda*, VITVI—*Vitis vinifera*, PICABHC—*Picea abies* (high-quality gene set), MIC—*Microlepia cf. marginata*, Pp—*Physcomitrium patens*, FUNHY—*Funaria hygrometrica*, SALCU—*Salvinia cucullata*, AZOFI—*Azolla filiculoides*, ANTQU—*Anthoceros agrestis*, KLEFL—*Klebsormidium nitens*, COLORtr—*Coleochaete orbicularis* (transcriptome-based), COLSPtr—*Coleochaete* sp. (transcriptome-based), SELMO—*Selaginella moellendorffii*). Red letters indicate the three *A. thaliana* DOG1 proteins. Green letters indicate the five DOG1-containing proteins in *P. patens*. Right panel: domain architecture of DOG1 proteins; DOG1: delay of germination 1; Ank_2: ankyrin 2 domain; Ank_4: ankyrin 4 domain; Ank_5 ankyrin 5 domain. Black line indicates full protein. (b) Alignment of *A. thaliana* and *P. patens* DOG1 domains. Using ClustalX 2.1 (Larkin et al., 2007), peptide sequences were taken from the Pfam database and aligned. Asterisks highlight positions which comprise a single, fully conserved residue, colons mark that one of the following conservative groups is fully conserved: STA, NEQK, NHQK, NDEQ, QHRK, MILV, MILF, HY or FYW. Dashes represent alignment indels.

Ppdog1-l1 mutant spores germinate faster than the control

To understand the influence of the *PpDOG1-L1* function on spore germination, we performed germination assays under long-day (LD) conditions. For this purpose, mature sporophytes (brown, according to Hiss, Meyberg, et al., 2017) were isolated 42 days after watering the gametangia (male antheridia and female archegonia) and incubated at 4°C for at least 2 weeks. We examined the germination of *Ppdog1-l1* and *Ppdog1-l1*:*AtDOG1* compared to the wild-type control (Reute ecotype).

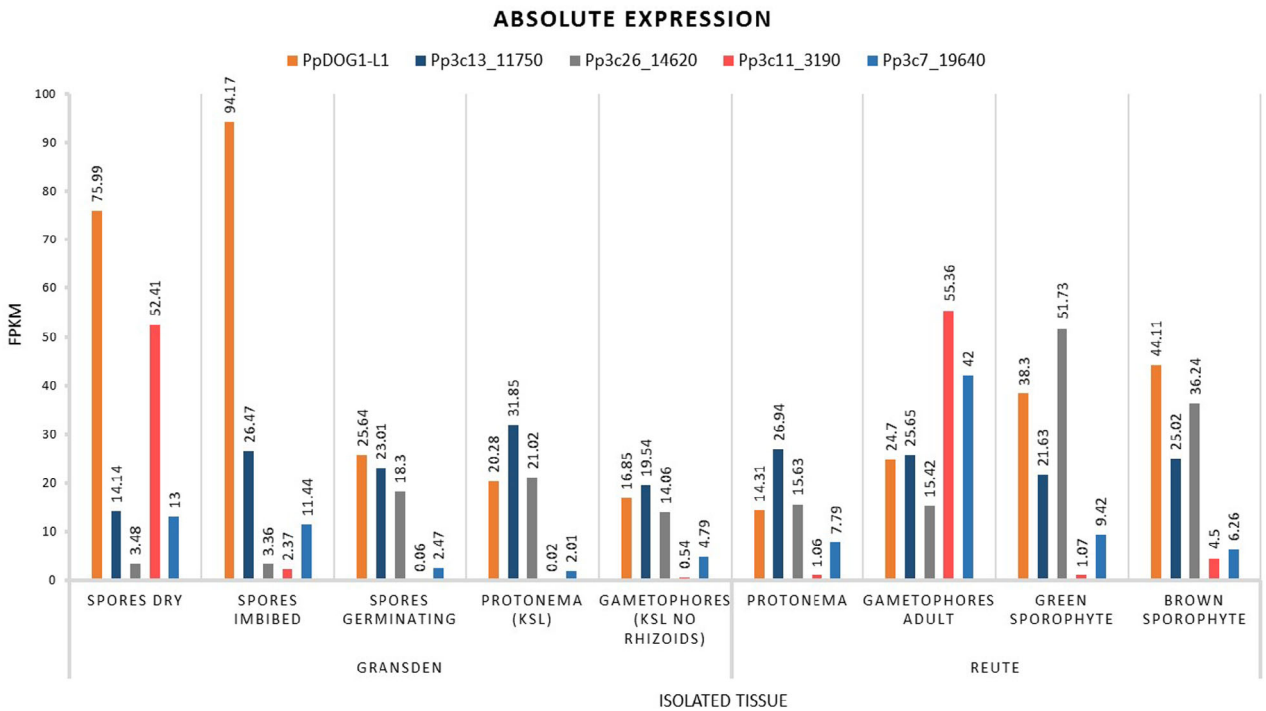

Figure 2. Expression analysis of DOG1-domain containing transcripts using PEATmoss database. Bar graph depicting PEATmoss [https://peatmoss.plantcode.cup.uni-freiburg.de/expression_viewer/input (Fernandez-Pozo et al., 2020)] absolute expression FPKM values of all five *DOG1*-like genes using RNAseq data of various developmental stages of *P. patens* ecotypes Gransden and Reute (Fernandez-Pozo et al., 2020; Perroud et al., 2018). FPKM, fragments per kilobase of exon per million mapped fragments; KSL, Knop solid.

Ppdog1-l1 spores germinated faster than the wild type in multiple experiments performed in two independent laboratories using different lighting conditions (Figure 4; Figures S4 and S5). However, the expression of *AtDOG1* in *Ppdog1-l1* yielded spores that germinated more slowly than the control (Figure 4).

In summary, *Pp*DOG1-L1 is important for the negative regulation of spore germination in *P. patens*. Moreover, *At*DOG1 can also function to restrain *P. patens* spore germination.

The DOG1 domain of *Pp*DOG1-L1 interacts in a yeast two-hybrid (Y2H) assay with the *Pp*DELLAa and *Pp*DELLAb proteins

Since *Ppdog1-l1*, *Ppdellaa*, *Ppdellab* and *Ppdellaab* showed a similar germination phenotype (Phokas et al., 2023), we wondered whether *Pp*DOG1-L1 protein could interact with *Pp*DELLAa and *Pp*DELLAb.

Using a Y2H approach, we examined whether *Pp*DELLAa (*Pp*3c19_8310) or *Pp*DELLAb (*Pp*3c22_7230) and the *Pp*DOG1-L1 interacted with each other. Therefore, we generated yeast vectors containing full-length *PpDOG1-L1* coding sequences fused to a DNA-binding domain (pGBKT7) and full-length *PpDELLA* coding sequences fused to the GAL4 activation domain (pGADT7). Expression and subsequent translation of the proteins in yeast were detected via Western blot targeting the fused MYC tag (Figure S6a; Phokas et al., 2023). After introducing both plasmids into a Y2H reporter strain, we observed growth for all combinations on selective media without *LEU* and *TRP*, indicating that both plasmids were present in the yeast (Figure S6b). Interestingly, on selective media lacking *ADE*, *HIS*, *LEU* and *TRP* we observed growth for the combinations of *Pp*DELLAa and *Pp*DELLAb with *Pp*DOG1-L1 (Figure 5a; Figure S6b).

Since *Pp*DOG1-L1 harbours a C-terminal ANK domain, we wanted to elucidate which domain, DOG1 or ANK, interacts with the *Pp*DELLA proteins. We generated truncated versions of the DOG1-like protein *Pp*DOG1-L1 that contain either the DOG1 or the ANK domain. Both truncated versions were expressed in yeast as evidenced by anti-MYC Western blots (Figure S6c) and all plasmids were successfully co-expressed as evidenced by growth on selective media without *LEU* and *TRP* (Figure S6d). For the DOG1-domain containing, truncated protein *Pp*DOG1-L1we observed an interaction with *Pp*DELLAb (Figure 5b). In contrast, no DELLA interaction with the ANK domain could be observed (Figure 5b; Figure S6d). In conclusion, the DOG1-domain of *Pp*DOG1-L1 was sufficient for *Pp*DELLAb interaction, but not for interaction with *Pp*DELLAa. This suggests that the combination of DOG1 and ANK domain may be important for the interaction of *Pp*DOG1-L1 with *Pp*DELLAa protein.

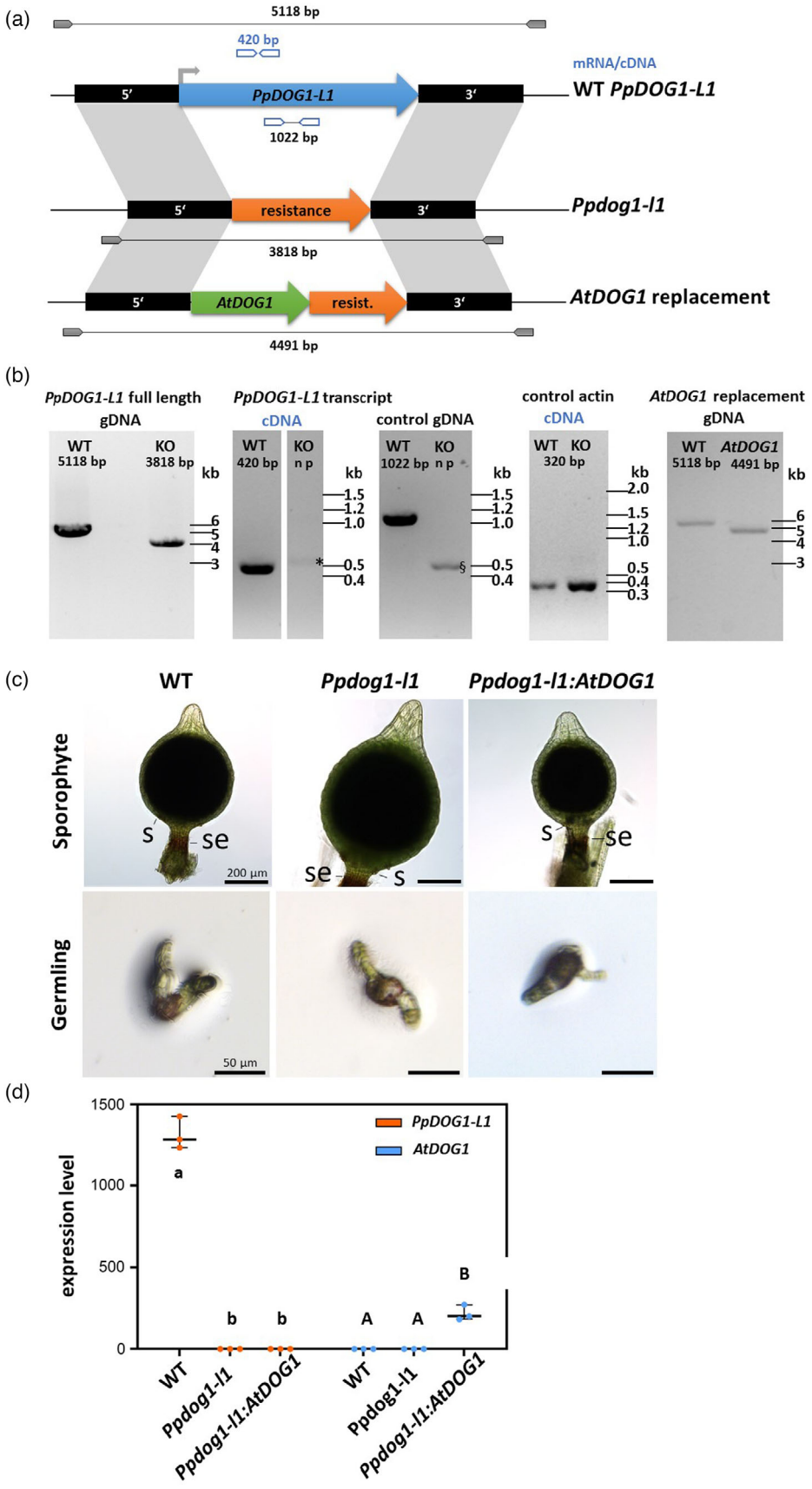

Figure 3. Characterisation of the *Ppdog1-l1* knockout strain and the *At*DOG1 replacement strain *Ppdog1-l1:AtDOG*. (a) Schematic representation of the *Pp*3c3_9650 (*PpDOG1-L1*) gene locus and knockout strategy. Black boxes indicate homologous recombination sites (LB, left border; RB, right border). The blue, orange and green arrows depict the *PpDOG1-L1* gene locus, hygromycin resistance cassette, and *Arabidopsis thaliana DOG1* (*AtDOG1*) gene, respectively. The angular grey arrow shows transcription start site for the mRNA (blue curved line). Small arrows show primer sites for gDNA full-length primer amplifying the integration locus (light grey) or cDNA (copyDNA) amplification (open blue boxes). PCR product sizes are depicted as numbers in base pairs (bp). (b) Genotyping of the *PpDOG1-L1* gene locus. Left panel image depicts full-length amplification of wild-type (WT) and knockout (KO) strains with primers 9650_outLB_FWD and 9650_outRB_REV (see Table S1). Middle panel images depict the amplification of a partial transcript, where primers are located in different exons of the gene (primers used: 9650_FWD and 9650_REV). In WT cDNA, the expected band size was 420 bp compared to KO cDNA with no specific product. As a control, WT gDNA amplified a 1022 bp product compared to KO gDNA with no specific product. The amplification of actin (*Pp*3c10_17080) served as a control for the cDNA with a product size of 320 bp for both WT and KO strains (primers used: ACTIN5_FWD and ACTIN5_REV). The rightmost image represents the full-length amplification of the replacement with *AtDOG1* (primers used: 9650_outLB_FWD and 9650_outRB_REV). np, no product; *, unspecific band; §, unspecific band of different size than in *. (c) Phenotyping of *Ppdog1-l1* and *Ppdog1-l1:AtDOG1* compared to wild type Reute (Re). All genotypes (wild type Re, *Ppdog1-L1* and *Ppdog1-l1:AtDOG1*) developed sporophytes showing normal development and no morphological differences. All sporophytes examined showed stomatal (s) development as well as seta browning (se) and spore development (dark area within the capsule). Spores of both mutants germinated (germlings) and showed the protrusion of one to two filaments 3 days after germination [compared to (Vesty et al., 2016)]. (d) qPCR results in wild type and both mutants using primers for *PpDOG1-L1* as well as for *AtDOG1* in gametophores grown for 4 weeks under long-day conditions. Expression level is relative to a thioredoxin control (Hiss, Meyberg, et al., 2017). Different letters indicate significant differences as determined by one-way ANOVA followed by post hoc Tukey's HSD test: *P*-adj. <0.05.

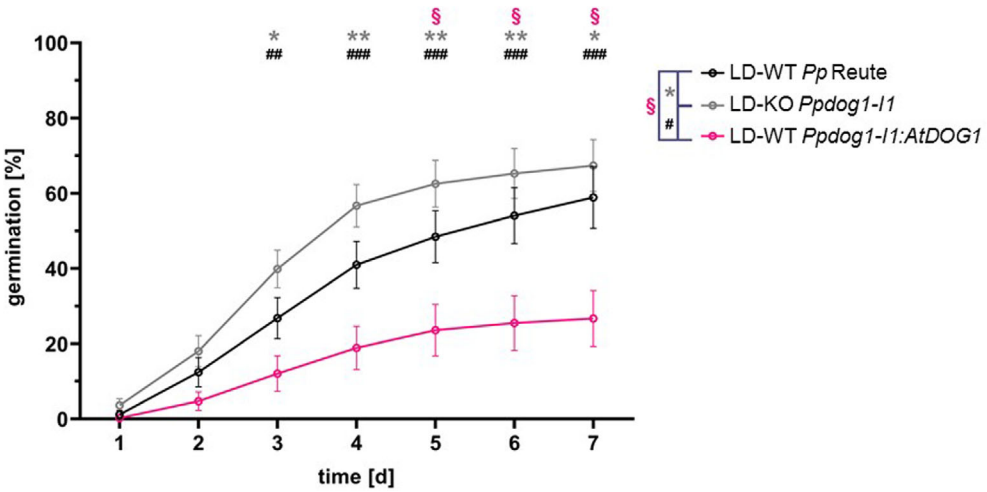

Figure 4. Germination rate determination under long-day conditions for *Ppdog1-l1* and *Ppdog1-l1:AtDOG1* compared to wild type. Diagram depicting germination rates of WT (black line), *Ppdog1-l1* (grey line), and *Ppdog1-l1:AtDOG1* (pink line) over 7 days. For germination of spores, long-day conditions were tested with $N \geq 3$. For each independent repetition of the experiment, three to five technical replicates were carried out. Statistical significance was calculated using the CountSpores R package. Lines depict estimated means ± SEM. $^{*/\S}P < 0.05$; $^{**/\#\#}P < 0.01$; $^{\#\#\#}P < 0.001$.

The DOG1-like protein *Pp*DOG1-L1 interacts with Arabidopsis DELLA protein *At*RGA

To better understand the lineage-specific evolution of DOG1 function, we examined whether the Arabidopsis DELLA protein *At*RGA can interact with *Pp*DOG1-L1 and whether *Pp*DELLA proteins can interact with *At*DOG1. Hence, we cloned the full-length *AtDOG1* coding sequence in pGBKT7, which was successfully expressed in yeast (Figure S7a). The presence of the protein was detected via Western blot using the MYC tag (Figure S7a). *AtRGA* in pGADT7 was provided (Yasumura et al., 2007). The presence of the vectors was detected by growth assays on selective media lacking *LEU* and *TRP* (Figure S7b). Similar to the first Y2H assay using *Pp*DELLAa or *Pp*DELLAb as bait, only yeast strains containing *At*RGA and *Pp*DOG1-L1 grew on selective media (Figure 5c; Figure S7b). However, no growth was observed for *Pp*DELLAa and *Pp*DELLAb as bait on depletion media when combined with *At*DOG1 as prey (Figure S7b). We additionally tested whether truncated versions of *Pp*DOG1-L1 containing only the DOG1 domain or the ANK domain could bind to *At*RGA. Neither the DOG1 domain nor the ANK domain was sufficient for interaction with *At*RGA (Figure S7c).

Overall, the full-length DOG1-like protein *Pp*DOG1-L1 interacted with DELLA protein *At*RGA from Arabidopsis, whereas the *At*DOG1 protein was unable to bind to DELLA proteins from *P. patens* in the yeast system. However, the DOG1 domain of *Pp*DOG1-L1 was insufficient for interaction with *At*RGA, suggesting that the ANK domain of the *Pp*DOG1-like protein is needed for its interaction with *At*RGA in yeast.

DISCUSSION

The understanding of evolutionary forces acting on the functions of conserved proteins of seed and non-seed

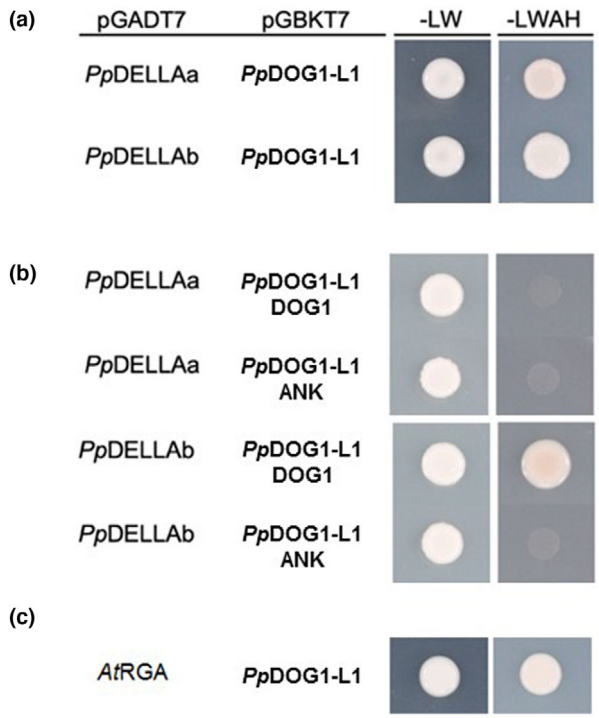

Figure 5. Yeast two-hybrid assays reveal interactions of *Pp*DOG1-L1 and DELLA proteins from *P. patens* and *A. thaliana*. (a) Yeast two-hybrid assay between *Pp*DOG1-L1 protein fused with the DNA-binding (DBD) domain in the pGBKT7 vector and *Pp*DELLAs fused with the GAL4 activation domain (AD) in pGADT7. *Pp*DELLAs interact with *Pp*DOG1-L1. Representative results of three biological replicates are shown. (b) Yeast two-hybrid assay between *Pp*DELLAs in pGADT7 and truncated *Pp*DOG1-L1 protein in pGBKT7. The DOG1 domain is necessary for interaction with *Pp*DELLAs and sufficient for interaction with *Pp*DELLAb. (c) Yeast two-hybrid assay between *At*RGA in pGADT7 and *Pp*DOG1-L1 protein in pGBKT7. *Pp*DOG1-L1 protein can interact with Arabidopsis DELLA protein *At*RGA. Representative results of three biological replicates are shown. DOG1, DOG1 domain; ANK, ankyrin repeats domain. Empty vector controls are shown in supplementary information (Figures S6 and S7).

plants is crucial to gain insights into the development and evolution of terrestrial plants. This information helps to address future questions about how plants can adapt to changes in, for example, temperature, nutrient supply or light conditions, such as through climate change. In this study, we used the model organism *Physcomitrium patens* to investigate the function and evolution of DOG1 proteins, which are known to play a key role in regulating seed germination in *A. thaliana* (Graeber et al., 2014), and are conserved among bryophytes (Nishiyama et al., 2021).

Three *P. patens* DOG1-like proteins possess DOG1 as well as ANK repeat domains

While DOG1 proteins in most seed plants contain only the DOG1 domain (Nishiyama et al., 2021), there are three types of DOG1 domain-containing proteins in non-seed plants: TGA-Rs, ANKYRIN (ANK) repeat domain-containing proteins, and DOG1 containing proteins with no additional domain. In *P. patens*, we identified five DOG1-like proteins, two of which contain only the DOG1 domain and three of which feature additional ANK domains. The combination of ANK and DOG1 domains seems to be unique to spore-bearing plants, indicating a specific function of the DOG1 protein in spore-bearing plants compared to seed plants such as *A. thaliana*. In a recent publication, the authors claimed that the evolutionary origin of *DOG1* genes may be *TGA*s (Nonogaki et al., 2022). In *P. patens*, four TGA proteins are present (Nishiyama et al., 2021).

The *P. patens* DOG1-like proteins that only contain the DOG1 domain are phylogenetically related to the ANK domain containing DOG1 proteins. ANK repeat domains are highly conserved and common in all kingdoms of life, including plants (Jernigan & Bordenstein, 2014; Mosavi et al., 2004). The structure of ANK repeat domains is well-characterised and is a common domain for protein–protein interactions (Bork, 1993). Their abundance in a large number of different proteins appears to be an evolutionary mechanism that enables novel functions through protein interaction (Mosavi et al., 2004).

The gene encoding the ANK-domain containing DOG1-like protein *Pp*DOG1-L1 is highly expressed in spores

In *A. thaliana*, DOG1-ABA-dependent seed dormancy is already present in developing seeds (Graeber et al., 2012). Expression of *DOG1* varies with the state of the seed and its abundance correlates with the depth of dormancy (Footitt et al., 2020). The mRNA level increases after pollination and peaks about 16 days after pollination (Nakabayashi et al., 2012). This fits with the mRNA expression pattern of *Pp*DOG1-L1 during sporophyte development, having its expression peak in mature/imbibed spores and lower expression in germinating spores, indicating a suppressive function in *P. patens* spores. In *A. thaliana*, there are three additional DOG1-like proteins: DOGL1 (DOG1-like, AT4G18660), DOGL2 (AT4G18680) and DOGL3 (AT4G18690) (Nishimura et al., 2018). Their expression is mainly observed in mature seeds (Berardini et al., 2015), but their function is diverse, such that increasing *DOGL3* expression promotes ABA hypersensitivity in seed germination, suggesting that DOG1 and DOG1-like proteins in *A. thaliana* are not redundant (Carrillo-Barral et al., 2020).

PpDOG1-L1 is involved in the control of spore germination and potentially in timing of sexual reproduction

As expected for deletion or loss-of-function mutants of DOG1 and related proteins in vascular plants, the deletion of *PpDOG1-L1* did not result in drastic phenotypic changes. Our analyses showed that gametangia of *Ppdog1-l1* might mature earlier than the wild type, which is especially visible when focusing on antheridia. Most of these antheridia have already released spermatozoids, whereas most

wild-type antheridia only have swollen tip cells (Hiss, Meyberg, et al., 2017). This fits with findings in lettuce where *dog1* suppression leads to an early flowering phenotype via control of miR172 (Huo et al., 2016). Interestingly, this miRNA can be found in *P. patens* (83% identical with *A. thaliana* sequence) and thus might be a conserved mechanism for the control of reproductive development in land plants.

With regard to spore germination, the deletion of *PpDOG1-L1* resulted in earlier germination as compared to the control. *At*DOG1 expressed in the *Ppdog*1-*l1* knock-out mutant reduced the number of germinating spores and delayed the germination process. These findings suggest conserved function of the DOG1 domain for control of germination. While we cannot exclude additional integration of both the knockout and replacement construct at additional sites in the genome influencing the phenotype, we show that the construct is integrated by homologous recombination into the correct locus, that the mRNA is not expressed in the mutant, and that the *AtDOG1* mRNA is expressed in the replacement line.

Interaction of DOG1 and DELLA proteins

In seed plants, the protein network featuring DOG1 includes important regulators of reproductive development such as, for example, DELLA and MOTHER OF FT and TFL1 (MFT) (Ali et al., 2022; Xi et al., 2010). DELLA proteins are well-known for interacting with many other proteins, mainly transcription factors, to regulate various developmental processes (Briones-Moreno et al., 2023; Lantzouni et al., 2020; Marin-de la Rosa et al., 2014). For example, in Arabidopsis, DELLAs interact with ABA-INSENSITIVE 3 (ABI3) and ABI5 to activate transcription of *SOMNUS* (SOM), repressing seed germination at high temperatures (Lim et al., 2013). In this study, we show that *Pp*DELLAa and *Pp*DELLAb as well as *At*RGA interact with the DOG1-like protein *Pp*DOG1-L1 in yeast. Hence, a similar mechanism as in seed plants might be active in *P. patens*, with *Pp*DOG1-like proteins potentially activating expression of downstream genes that promote spore dormancy. As there is no evidence that DOG1 proteins function as transcription factors, it is possible that the *Pp*DELLA-*Pp*DOG1-like interaction could involve the formation of a complex with a transcription factor, which activates dormancy-promoting gene expression. Alternatively, *Pp*DELLAs and the *Pp*DOG1-like protein might be forming part of a transcription-repressing complex that hinders activation of spore germination-promoting gene expression (Phokas & Coates, 2021). This mechanism has previously been shown for *At*DELLA proteins, which form a protein complex with BOTRYTIS SUSCEPTIBLE1 INTERACTOR (BOI) to inhibit seed germination, among other developmental processes (Park et al., 2013).

Protein–protein interaction in our yeast two-hybrid analyses revealed that the interaction of *Pp*DELLAa, *Pp*DELLAb and *At*RGA occurred with the *Pp*DOG1-like protein *Pp*DOG1-L1 harbouring ANK domains. The DOG1 domain of *Pp*DOG1-L1 was necessary for interaction with all DELLA proteins tested. The ANK domain of *Pp*DOG1-L1 by itself was not sufficient for the interaction with *P. patens* or Arabidopsis DELLA proteins but was necessary for interaction with *Pp*DELLAa and *At*RGA. The DOG1 domain of *Pp*DOG1-L1 by itself was only sufficient for interaction with *Pp*DELLAb.

*At*DOG1, which has no ANK domain, could not interact with DELLA proteins in yeast. This suggests functional divergence of *P. patens* and *A. thaliana* DOG1-like proteins rather than DELLAs. Moreover, expression of *AtDOG1* in the *Ppdog1-l1* knockout mutant restrained spore germination to below wild-type levels. Together these data suggest a possible DELLA-independent action of *At*DOG1 in *P. patens*. For example, *At*DOG1 might regulate *PpDELLA* downstream targets that promote inhibition of spore germination.

Conclusion and outlook

We conclude that a DOG1-like protein in *P. patens* restrains spore germination and may have different interaction partners than the flowering plant *At*DOG1 protein.

Hence, intriguingly, the function of DOG1 proteins in controlling the germination of dispersal structures appears to have been conserved since the earliest land plants. The interaction with GRAS proteins that harbour a DELLA domain might also be an ancestral state—however, this interaction has obviously diverged, since cross-lineage interaction of DOG1 and DELLA domains could not be detected in this study. The ANK domains present in the non-seed plant DOG1-like protein may stabilise DOG1-like-DELLA interactions and might additionally be required for non-DELLA protein–protein interactions, involving mechanisms that have been replaced or lost during seed plant evolution.

EXPERIMENTAL PROCEDURES

Phylogeny, gene model, domain and in silico expression analyses

Protein sequences were harvested using BLASTP with *At*DOG1 as query. Sequences were aligned using Mafft v7.310 in the auto mode (Katoh & Standley, 2013). Alignments were manually curated using Jalview 2.8 (Waterhouse et al., 2009). The best suited amino acid substitution model was determined using ProtTest 3.4 (Darriba et al., 2011) and turned out to be JTT. Bayesian inference utilising MrBayes 3.2.5 (Ronquist et al., 2012) was carried out with two hot and cold chains until the average standard deviation of split frequencies was below 0.01 (191 600 generations) and no more trend was observable; 250 trees each were discarded as burn-in. Trees were visualised using FigTree (http://tree.bio.ed.ac.uk/software/figtree/). Domain composition was analysed and visualised on the tree using DoMosaics (Moore et al., 2014).

For the *P. patens* v3.3 gene model *Pp*3c26_14620V3.1 there is evidence of alternative splicing. There is an older (v3.1) gene model that is representative of this splice form (Figure S1).

Indeed, amplification of the transcripts yielded amplicons of different size, and analysis of RNA-seq data using the Tablet graphical viewer for sequence assemblies and alignments (Milne et al., 2013) confirmed a short splice variant lacking the ANK (ankyrin repeat) domains. Since there was evidence for ANK-containing proteins in all non-seed plant lineages except club mosses, the *Selaginella moellendorffii* gene models were manually inspected. An alternative gene model (to JGI ID 173073) was found that features ANK domains C-terminal of the DOG1 domain (cf. XM_024677809.1, NCBI; Figure S1). In both cases, both variants were included for alignment and tree generation.

Amino acid sequences of *A. thaliana* and *P. patens* DOG1 domains were taken from Pfam database (PF14144) and aligned using ClustalX 2.1 (Larkin et al., 2007).

Gene expression of *P. patens* ecotypes Gransden and Reute were analysed using the developmental stages dataset of the PEATmoss webtool (https://peatmoss.plantcode.cup.uni-freiburg.de/) (Fernandez-Pozo et al., 2020).

Putative localization of DOG1 proteins was predicted using the green targeting predictor [GTP_Pp (Fuss et al., 2013)] using *P. patens* data. The significance cut-off is described as 0.5 (https://plantcode.cup.uni-freiburg.de/plantco/predloc/).

Vector construction for knockout in *P. patens*

The *PpDOG1-like 1* (*PpDOG1-L1*; *Pp*3c3_9650V3.1) knockout vector was generated as follows: homologous regions (left border LB; right border RB) for recombination were amplified with Phusion High-Fidelity DNA Polymerase [New England Biolabs (NEB), Ipswich, UK] from gDNA of *P. patens* using the following primers: 9650_HinDIII_LB_FWD, 9650_LB_XhoI_REV; 9650_SpeI_RB_FWD and 9650_RB_AscI_REV (Table S1). Ligation in pJET-1.2 was done as previously described. Restriction digestion of the two homologous regions and pBHRF-containing hygromycin resistance cassette (Schaefer et al., 2010), extraction of the correct bands by gel purification, and ligation with T4 DNA ligase (New England Biolabs) according to the manufacturer's instructions with transformation in TOP10 *E. coli* (Thermo Fisher Scientific, Waltham, MA, USA) were performed.

For replacement of *PpDOG1-L1* with *At*DOG1 in the knockout strain *Ppdog1-l1*, the AT5G45830 cDNA sequence was amplified from cDNA of *A. thaliana* seeds as described in the RNA isolation and cDNA synthesis section and cloned in pJET-1.2. The primers used were: AT5G45830_AscI FWD and AT5G45830_AscI REV (Table S1). Homologous regions for integration into the knockout locus were amplified from gDNA of the knockout strain with the following primers: 9650_ApaI_LB FWD, 9650_LB_AscI REV, 9650_NdeI_RB and 9650_RB_NotI REV (Table S1). Restriction and ligation were performed using pBSD containing a blasticidin resistance cassette (Ishikawa et al., 2011) as the final vector.

All plasmids were checked by sequencing.

Quantification of transcript levels

Gametophores of *P. patens* ecotype Reute, *Ppdog1-l1*and the *Ppdog1-l1* mutant expressing *A. thaliana DOG1* (*Ppdog1-l1*: *AtDOG1*) were incubated on solid Knop's medium under long day conditions (16/8 h light/dark, temperature: 24 ± 1°C, light intensity: ~50 µmol m^{-2} sec^{-1}) for 4 weeks. Total RNA of gametophores was extracted using PureLink (TM) Plant RNA Reagent (Thermo Fisher Scientific; Cat. No. 12322–012), followed by RNA clean up using RNAll plant RNA kit (Bioline Meridian Bioscience, London, UK). RNA concentration was determined using a NanoDrop ND-8000 UV–Vis spectrophotometer (Thermo Fisher scientific). RNA (1 µg) was reverse transcribed to cDNA using the High-Capacity Reverse Transcription Kit (Thermo Fisher Scientific; Cat. No. 4368814), and qRT-PCR was performed using the SensiFAST™ SYBR Hi-ROX kit (Bioline Medidian Bioscience, London, UK; Cat. no. BIO-92005). Experiment was performed in triplicate with three biological replicates. Gene expression levels were normalised to a thioredoxin control. Primers used for qRT-PCR can be found in Table S1.

Plant material and culture conditions, transfection

P. patens ecotype Reute (Hiss, Schneider, et al., 2017) was used to generate the knockout mutant. Gametophore *in vitro* cultures were grown in 9 cm Petri dishes with Knop's medium (Knop, 1868) for 4 weeks under long-day conditions [LD; 22°C, 16 h: 8 h, light: dark, (Hiss, Schneider, et al., 2017)]. Plates were initially sealed with 3M micropore tape (3M Healthcare, Neuss, Germany) for 1 week to promote development. Afterwards, the plates were sealed with parafilm. For gametangia induction, *in vitro* gametophore cultures were incubated for 3 weeks under short-day conditions (SD; 15°C, 8 h: 16 h, light: dark, 20 µmol m^{-2} sec^{-1}). Sporophyte development was initiated by irrigation with 2–3 ml sterile tap water. Mature sporophytes developed after approximately 42 days.

Transient transfection of *P. patens* was performed as previously described (Hiss, Schneider, et al., 2017). To establish stable transformants, the protocol for transient transfection was used with the following changes: a linearized construct [enzymes used AscI (NEB) and BlnI (Takara Bio Europe, Saint Germain en Laye, France)] and 4 ml of regeneration medium were used. Two rounds of selection were performed on Knop's medium plates supplemented with 20 µg ml^{-1} hygromycin, with intervening selection releases for regeneration on non-supplemented medium.

Genomic DNA isolation and genotyping

The Dellaporta protocol with modifications as previously described was used to isolate genomic DNA (Dellaporta, 1983; Hiss, Meyberg, et al., 2017).

For genotyping, Q5 High-Fidelity DNA polymerase (NEB) was used as described in the manufacturer's instructions with the following primers: 9650_outLB FWD; CamvTer FWD; 9650_outRB_REV; 9650_midLB_FWD and 35s REV (Table S1).

RNA isolation and cDNA synthesis from *P. patens* and *A. thaliana* tissue

RNA isolation from *P. patens* tissue was performed with the RNeasy Plant Mini Kit (Qiagen, Hilden, Germany) according to the manufacturer's instructions using a mortar and pestle and with the following additional step. After centrifugation in the pink column, we performed DNase digestion with RNase-free DNase Set (Qiagen) according to the manufacturer's instructions. RNA quality and quantity were checked using the Nanodrop 1000 ND-1000 Spectrophotometer Microvolume (Thermo Fisher Scientific).

RNA isolation from *A. thaliana* seeds was performed by the CTAB method as follows. 100 mg seeds were frozen in liquid nitrogen and ground with a mortar and pestle. The powder was mixed with CTAB buffer [2% (w/v) hexadecyl-trimethyl-ammonium bromide, 2% polyvinylpyrrolidone, 2 M NaCl, 100 mM Tris–HCl pH8, 20 mM EDTA, 2% β-mercaptoethanol] and incubated at 65°C for 10 min with repeated shaking. RNA was extracted by adding chloroform/isoamyl alcohol (24:1) and centrifuging three times at 12 000 ***g*** for 10 min at room temperature. To the aqueous phase, 0.25 vol. 10 M lithium chloride was added and incubated overnight at 4°C. After centrifugation at 14 000 ***g*** for 20 min at 4°C, the pellet

was resuspended in SSTE buffer (1 M NaCl, 0.5% SDS, 10 mM Tris–HCl pH8, 1 mM Na_2EDTA). After another three times extraction with chloroform/isoamyl alcohol (24:1), ethanol (96%) was added, incubated for 2 h at 4°C and centrifuged for 30 min at 4°C. This was followed by a wash step with 80% ethanol, and the final RNA pellet was resuspended after air-drying. DNA was removed by addition of RNase-free DNase Set as previously described and processed with RNA Cleanup (Qiagen) according to the manufacturer's instructions.

Reverse transcription was performed using the SuperScript III First-Strand Synthesis System (Thermo Fisher Scientific) according to the manufacturer's instructions. Random Primer Mix (New England Biolabs) was used. PCR amplification was performed using Q5 polymerase according to the manufacturer's instructions with the following primers: *Pp*3c10_17080V3.1 *ACTIN5* FWD and REV as well as *Pp*3c3_9650V3.1 9650_FWD and REV (Table S1).

P. patens phenotyping

Microscopic analysis of protonemal growth during spore germination was performed as described for the germination assay. After 3 days, germlings were analysed on plate using an S8 Apo binocular equipped with a MC170 HD camera, Leica Application Suite 4.4 (LAS, Leica, Wetzlar, Germany). For gametangia development, plates were transferred to SD as described above and gametangia were analysed 21 days after induction. For microscopic documentation, apices were prepared using the Leica S8 Apo and freed from leaflets using forceps. Gametangia were transferred into sterile tap water on microscopy slides and covered with coverslips. Images were done using the Leica DM6000 as described above.

Sporophytes were induced as described above and microscopic analysis was performed on brown sporophytes (Hiss, Meyberg, et al., 2017), using the Leica DM6000 as described above (Leica, Wetzlar, Germany). Mature spores were submerged in sterile tap water and analysed using oil-immersion.

Microscopic analyses and image processing

Transformed *P. patens* protoplasts were examined with confocal laser scanning microscopes (TCS SP2: upright Leica DM RE type 13 TL.HC RF 4, HC E.VIS; TCS SP5: upright Leica DM6000 B with motorised x,y-stage). Images of developmental stages were taken at 1024 × 1024 pixels and processed with ImageJ/Fiji (version 2). The Leica S8 Apo binocular was used to study the phenotypes. The binocular was controlled via the Leica Application Suite version 4.4. Brightness and contrast were adjusted using Microsoft Power Point (Microsoft, Redmond, WA, USA). Analyses of cell composition and numbers of 7-day-old protonema grown from germlings was done using ImageJ Version 1.53c (http://imagej.nih.gov/ij). Statistical analysis was carried out using Microsoft Excel 2019 (Microsoft).

Germination assays

Germination assays were performed after (Vesty et al., 2016). After 2 weeks at 4°C, mature sporophytes were squeezed in 500 µL of sterile distilled water to release spores. The spore suspension was pipetted onto plates containing Knop's medium supplemented with 8.4 mM ammonium tartrate and microelement solution (50 µmol L^{-1} H_3BO_3, 50 µmol L^{-1} $MnSO_4 \times H_2O$, 15 µmol L^{-1} $ZnSO_4 \times 7\ H_2O$, 2.5 µmol L^{-1} KI, 0.5 µmol L^{-1} $Na_2MoO_4 \times 2\ H_2O$, 0.05 µmol L^{-1} $CuSO_4 \times 5\ H_2O$, 0.05 µmol L^{-1} $Co(NO_3)_2 \times 6\ H_2O$). For each germination assay, a minimum of three independent biological replicates were analysed with five sporophytes per mutant/control and five technical replicates each. Spores were age-matched between wild type and transgenic lines, using spores harvested in the same time range from plants grown under the same conditions. Incubation was performed under LD conditions with different light sources (LED and fluorescent bulbs) and in different labs as indicated in respective figure legends. Counting of germination events was carried out daily for a total of 7 days with Leica S8 Apo Binocular microscope.

Statistics on germination

To account for the different number of spores in different plants, we analysed the relative number, that is the number of germinated spores per segment of the plate (e. g. 1/16) divided by the total number of spores per segment. The number of germinated spores per segment roughly ranged from 50 to 5000. To confirm that such relative count data can be analysed by statistical models assuming a normal distribution, we performed simulation studies and evaluated the distribution of the data using quantile-quantile plots. The total number of germinated spores per plate was drawn from a Poisson distribution and randomly assigned to one out of 16 segments. Then, the counts in each segment were normalised by the total number of spores per plate and the distribution of the residuals was compared to the normal distribution by quantile-quantile plots, showing no obvious deviations.

A mixed effects model,

$$Y_{ctps} = T_t + C_c + D_{ct} + P_{ctp} + \varepsilon_{ctps} \text{ with } \varepsilon_{ctps} \sim N\left(0, \sigma^2\right), P_{\text{ctp}} \sim N\left(0, \sigma'^2\right),$$

was applied to account for biological variability σ'^2 between plants $p = 1, \ldots, N$ and variabilities σ^2 between the three segments $s = 1,2,3$ of one plate. Y_{ctps} denotes the measured normalised counts for condition c at time point t on plate p in segment s. T_t refers to the estimated main effects over time. D_{ct} denote interaction terms, that is, differences between the reference condition $c = 1$ and other conditions $c > 1$ at time point t, which were tested for significant deviations from zero.

We implemented this statistical analysis procedure in the R package CountSpores which is publicly available at github.com/kreutz-lab/CountSpores. Using the lme4 package for mixed-effects models, our package enables user-friendly analyses of similar data sets, provides example data, as well as functionality for plotting, testing interactions at individual time points and over entire time courses.

Generation of yeast two-hybrid constructs

P. patens RNA was extracted from gametophore tissue of Gransden (Gd) ecotype as described previously (Vesty et al., 2016). *P. patens* cDNA was then synthesised using the Tetro cDNA synthesis kit (Bioline, London, UK) with oligo(dT) primers as per manufacturer's instructions. Arabidopsis RNA was extracted from seedlings of Col-0 ecotype and used to synthesise cDNA as described previously (Labandera et al., 2021).

PpDOG1-L1 coding sequence (excluding start codon) was PCR-amplified from *P. patens* cDNA using *NdeI-Pp3c3_9650_F* with *SalI-Pp3c3_9650_R*. The PCR product was then ligated into pCR-blunt using the Zero Blunt PCR cloning kit (Thermo Fisher Scientific, Waltham, MA, USA) as per manufacturer's instructions, and sequenced (Eurofins, Wolverhampton, UK) using the primers *M13_F* and *M13_R*, before being digested out of pCR-blunt using *Nde*I and *Sal*I and ligated into pGBKT7 (Clontech, Takara Biosciences Europe, Saint Germain en Leye, France). Truncated *PpDOG1-L1* sequences encoding either the DOG1 or ANK domain were amplified from pGBKT7 containing the *PpDOG1-L1* coding sequence. For

Primers *NdeI-Pp3c3_9650_F* and *SalI-Pp3c3_9650_DOG_R* were used to amplify the DOG1 domain (encoding amino acids 1–296), while primers *NdeI-Pp3c3_9650_ANK_F* and *SalI-Pp3c3_9650_R* were used to amplify the ANK domain (encoding amino acids 297–531). The PCR products were digested using *Nde*I and *Sal*I and directly ligated with digested pGBKT7. Plasmids were then sequenced (Eurofins) to confirm integration of truncated coding sequences using a T7 primer.

The *AtDOG1 (AT5G45830)* coding sequence (excluding the start codon) was PCR-amplified from Arabidopsis cDNA using the primers *NdeI-AtDOG1_F* and *EcoRI-AtDOG1_R*. The PCR product was directly digested using NdeI and EcoRI, ligated with pGBKT7 and sequenced (Eurofins) using primers *T7_F* and *M13_R*. *PpDELLAa, PpDELLAb* and *AtRGA* cloned in pGADT7 (Yasumura et al., 2007) were kindly provided by Professor Nicholas Harberd, University of Oxford, UK. Primers are listed in Table S1.

Yeast protein expression, Western blotting and yeast two-hybrid assay

Yeast was grown overnight in liquid cultures of synthetic amino acid Drop out (DO) -leu-trp at 30°C. The OD_{600} of yeast cells was adjusted to 8 and centrifugation of 1 ml of culture was performed at 12 000 ***g*** for 4 min. The pellet was resuspended in 50 µl Buffer A (0.1 M NaOH, 50 mM EDTA, 2% SDS, 2% β-mercaptoethanol) and then incubated at 90°C for 10 min. 0.67 µl 3 M acetic acid was added to the suspension before shaking on a Titertek for 30 sec, followed by shaking for 1 min and then incubation at 90°C for 10 min. 12.5 µl of Buffer B (250 mM Tris pH 6.8, 50% glycerol, 0.05% bromophenol blue) was added to the suspension, followed by vortexing for 2 sec and centrifugation at 12 000 ***g*** for 5 min. 55 µl supernatant was then transferred to a clean tube and boiled for 1 min at 98°C. The final extract was either stored at −20°C or analysed directly via Western blotting.

Western blotting and yeast two hybrid including transformation of Matchmaker (AH109) yeast was performed as described in Bailey et al. (2021) and Phokas et al. (2023). Briefly, for yeast transformation, single colonies cultured on YPAD agar medium (20 g L^{-1} bacto-peptone, 10 g L^{-1} bacto-yeast extract, 20 g L^{-1} dextrose, 40 mg L^{-1} adenine sulfate, 20 g L^{-1} bacto-agar) were resuspended in 100 µl transformation buffer (2:1 50% PEG 3350MW, 1 M lithium acetate, 0.6% β-mercaptoethanol). 2 µg of each plasmid containing the construct of interest was added to the mixture and incubated at 37°C for 45 min on an orbital shaker (200 rpm), before being plated on DO -leu-trp medium to select for co-transformed plasmids. Plates were sealed with micropore tape (3M Healthcare) and incubated inverted at 30°C for 2–4 days. Following successful transformation, colonies were picked up, diluted in 150 µl nuclease-free water and 5 µl of the dilution was transferred onto DO-ade-his-leu-trp and DO-leu-trp plates in triplicates. The plates were incubated inverted at 30°C for 2–7 days and then photographed using a Nikon D40 SLR camera. For Western blotting, mouse monoclonal α-HA (Abcam, Cambridge, UK; ab130275) and α-MYC (Abcam, ab18185) were used at 1:2000 dilution in 10 ml 5% (w/v) Marvel semi-skimmed milk in TBST (50 mM Tris, 150 mM NaCl, pH 7.5 with 1 M HCl, 0.1% tween) and incubations were carried out for 3 h for α-HA and 1 h for α-MYC at room temperature or overnight at 4°C. Goat anti-mouse immunoglobin (Abcam, ab6789) was used as secondary antibody at a 1:2000 dilution in 5% (w/v) milk in TBST and was incubated for 1.5 h.

AUTHOR CONTRIBUTIONS

EV, AP, RM, CB, MP, MG, CG, PFP, KKU and JY performed research. EV, AP, RM, CB, MP and JY analysed data. EV, AP, RM, CB, MP and JY visualised data. EK, CK, JCC, SAR and AH provided resources. CK, JCC, SAR and AH provided funding acquisition. CG, RM, JCC, SAR, AH designed research. EV, CG, RM, CK, JCC, SAR, and AH supervised part of the project. EV, RM, CB, AP, JCC, and SAR wrote the manuscript. All authors reviewed the manuscript.

ACKNOWLEDGEMENTS

We thank Yuki Yasumura, Eric Belfield and Nicholas Harberd (University of Oxford) for contributing *Pp*DELLA and *At*RGA yeast two-hybrid constructs. We thank all lab members, former and present, for their support and discussion. Open Access funding enabled and organized by Projekt DEAL.

FUNDING INFORMATION

This project was carried out in the framework of MAdLand (http://madland.science, DFG priority program 2237), and SAR and AH are grateful for funding from the DFG (RE 1697/15-1, 20-1; HI 1369/8-1). This work is part of the ERA-CAPS SeedAdapt consortium (www.seedadapt.eu) and was supported by the German Research Foundation (grant no. RE 1697/8-1 to S.A.R.) C.K. and A.H. were supported under Germany's Excellence Strategy (EXC-2189—Project ID 390939984), A.P. was supported by the UK Biotechnology and Biological Sciences Research Council (BBSRC) doctoral training grant BB/M01116X/1.

CONFLICT OF INTEREST

The authors declare no conflict of interest.

SUPPORTING INFORMATION

Additional Supporting Information may be found in the online version of this article.

Figure S1. Comparison of gene model/splice variants of *P. patens* and *S. moellendorffii DOG1* genes. Variants w/ and w/o ANK domain maybe derived from intron retention. Schematic representation of *Pp*3c26_14620V3.1 coding sequences compared to *Selaginella moellendorfii* (SELMO) gene 173073 (JGI, Joint Genome Institute) as well as its NCBI entry XM _024677809.1. Green and blue bars represent coding sequences. AA, amino acid. Both variants of the *P. patens* transcript can be experimentally detected.

Figure S2. *In silico* expression analyses of *P. patens DOG1* homologous genes. PEATmoss (https://peatmoss.plantcode.cup.uni-freiburg.de/expression_viewer/input; Fernandez-Pozo et al. 2020) expression images depict FPKM values of all five DOG1 homologous genes using RNAseq data of various developmental stages of *P. patens* ecotypes Gransden and Reute. WT, wild type.

Figure S3. Gametangia development of *Ppdog1-l1*and *Ppdog1-l1*: *AtDOG1*compared to wild type Reute (WT) 21 days after induction. Immature: Apices with immature archegonia (female, tip cell closed, *) and mature antheridia (male, yellow to brownish colour, swollen and/or burst tip cells, a). Mature: Apices possess at least one mature archegonium (tip cell open, *) and mature antheridia (a). Fertilized: The archegonial neck canal (nc) cells are brownish, the venter is swollen and an embryo develops (e). Antheridia: Mature antheridia with swollen tip cell are visible for all strains

(arrow). *Ppdog1-l1* antheridia are mainly empty and degrade after spermatozoid release (*).

Figure S4. Germination rate determination under long-day conditions for *Ppdog1-l1* and *Ppdog1-l1:AtDOG1* compared to wild type. Diagram depicting germination rates of WT (black circles), knockout (grey circles), and replacement (pink circles) strains of *Pp*DOG1-L1 over seven days. For germination of spores, long-day conditions were tested using ≥3 repetitions and different light sources (LED and fluorescent bulbs for white light). For each independent repetition of the experiment, three to five replicates were tested. Statistical significance was calculated using CountSpores R package. Lines depict the estimated means ± SEM; $^{*/\S}P < 0.05$; $^{**/\#\#}P < 0.01$; $^{\#\#\#}P < 0.001$. *X*-axis: days; *Y*-axis: % germination.

Figure S5. *Ppdog1-l1* mutant spores germinate faster than wild type in a second lab environment. Spores of the knockout strain *Ppdog1-l1* germinate significantly faster than wild type (WT, Reute ecotype) spores. Error bars, ±SEM. Significant differences between knockout strain KO_*Pp*3c3_9650 and WT were tested using CountSpores R package. Representative of 3 biological repeats; means are the average of 3 technical replicates. $^{**}P < 0.01$, $^{***}P < 0.001$.

Figure S6. Immunoblot and yeast two hybrid approaches.

Controls linked to Figure 5. (a) MYC-tagged *Pp*DOG1-L1 (60kDa) was expressed in yeast cells (anti-MYC western blot). CBB, Coomassie brilliant blue staining. (b) No autoactivation in the yeast system is seen with *Pp*DELLAs or *Pp*DOG1-L1 coexpressed with empty vector controls. (c) MYC-tagged truncations of the *Pp*DOG1-like protein *Pp*DOG1-L1 harbouring either the DOG1 or ANK domain were expressed in yeast as detected by an anti-MYC western blot. CBB, Coomassie brilliant blue staining. (d) No autoactivation is seen in the yeast system with truncated *Pp*DOG1-L1 coexpressed with empty pGADT7 vector.

Figure S7. *At*DOG1 cannot interact with DELLA proteins and *At*RGA cannot interact with truncated DOG1 or ANK domains of *PpDOG1-L1*. (a) Anti-MYC western blot showing that MYC-tagged *At*DOG1 (34kDa) is expressed in yeast cells. Myc-tagged *Pp*DELLAa and *Pp*DELLAb as well as *At*RGA expression was shown elsewhere (Phokas et al. 2023). CBB, Coomassie brilliant blue staining. (b) Yeast two-hybrid assay between *At*RGA or *Pp*DELLAs in pGADT7 and *At*DOG1 in pGBKT7 plus empty vector controls. *At*RGA and *Pp*DELLAs do not interact with *At*DOG1. Representative results of three biological replicates are shown. (c) Yeast two-hybrid assay between *At*RGA in pGADT7 and truncated *Pp*DOG1-L1 in pGBKT7. Representative results of three biological replicates are shown. DOG1, DOG1 domain; ANK, ankyrin repeats domain.

Table S1. Primers used.

REFERENCES

Ali, F., Qanmber, G., Li, F. & Wang, Z. (2022) Updated role of ABA in seed maturation, dormancy, and germination. *Journal of Advanced Research*, **35**, 199–214.

Ashikawa, I., Abe, F. & Nakamura, S. (2013) DOG1-like genes in cereals: investigation of their function by means of ectopic expression in Arabidopsis. *Plant Science*, **208**, 1–9.

Bailey, M., Ivanauskaite, A., Grimmer, J., Akintewe, O., Payne, A.C., Osborne, R. *et al.* (2021) The Arabidopsis NOT4A E3 ligase promotes PGR3 expression and regulates chloroplast translation. *Nature Communications*, **12**, 251.

Becerra, C., Jahrmann, T., Puigdomenech, P. & Vicient, C.M. (2004) Ankyrin repeat-containing proteins in Arabidopsis: characterization of a novel and abundant group of genes coding ankyrin-transmembrane proteins. *Gene*, **340**, 111–121.

Bentsink, L., Jowett, J., Hanhart, C.J. & Koornneef, M. (2006) Cloning of DOG1, a quantitative trait locus controlling seed dormancy in Arabidopsis. *Proceedings of the National Academy of Sciences of the United States of America*, **103**, 17042–17047.

Berardini, T.Z., Reiser, L., Li, D., Mezheritsky, Y., Muller, R., Strait, E. *et al.* (2015) The Arabidopsis information resource: making and mining the "gold standard" annotated reference plant genome. *Genesis*, **53**, 474–485.

Bork, P. (1993) Hundreds of ankyrin-like repeats in functionally diverse proteins: mobile modules that cross phyla horizontally? *Proteins*, **17**, 363–374.

Briones-Moreno, A., Hernandez-Garcia, J., Vargas-Chavez, C., Blanco-Tourinan, N., Phokas, A., Urbez, C. *et al.* (2023) DELLA functions evolved by rewiring of associated transcriptional networks. *Nature Plants*, **9**, 535–543.

Carrera-Castano, G., Calleja-Cabrera, J., Pernas, M., Gomez, L. & Onate-Sanchez, L. (2020) An updated overview on the regulation of seed germination. *Plants (Basel)*, **9**, 703.

Carrillo-Barral, N., Rodriguez-Gacio, M.D.C. & Matilla, A.J. (2020) Delay of Germination-1 (DOG1): a key to understanding seed dormancy. *Plants*, **9**, 480.

Cheng, H., Qin, L., Lee, S., Fu, X., Richards, D.E., Cao, D. *et al.* (2004) Gibberellin regulates Arabidopsis floral development via suppression of DELLA protein function. *Development*, **131**, 1055–1064.

Darriba, D., Taboada, G.L., Doallo, R. & Posada, D. (2011) ProtTest 3: fast selection of best-fit models of protein evolution. *Bioinformatics*, **27**, 1164–1165.

Daviere, J.M. & Achard, P. (2013) Gibberellin signaling in plants. *Development*, **140**, 1147–1151.

Dekkers, B.J., He, H., Hanson, J., Willems, L.A., Jamar, D.C., Cueff, G. *et al.* (2016) The Arabidopsis DELAY OF GERMINATION 1 gene affects ABSCISIC ACID INSENSITIVE 5 (ABI5) expression and genetically interacts with ABI3 during Arabidopsis seed development. *The Plant Journal*, **85**, 451–465.

Dellaporta, S.L. (1983) A plant DNA minipreparation: version II. *Plant Molecular Biology Reporter*, **1**, 19–21.

Fernandez-Pozo, N., Haas, F.B., Meyberg, R., Ullrich, K.K., Hiss, M., Perroud, P.F. *et al.* (2020) PEATmoss (Physcomitrella Expression Atlas Tool): a unified gene expression atlas for the model plant *Physcomitrella patens*. *The Plant Journal*, **102**, 165–177.

Finch-Savage, W.E. & Leubner-Metzger, G. (2006) Seed dormancy and the control of germination. *The New Phytologist*, **171**, 501–523.

Footitt, S., Walley, P.G., Lynn, J.R., Hambidge, A.J., Penfield, S. & Finch-Savage, W.E. (2020) Trait analysis reveals DOG1 determines initial depth of seed dormancy, but not changes during dormancy cycling that result in seedling emergence timing. *The New Phytologist*, **225**, 2035–2047.

Fu, X., Richards, D.E., Ait-Ali, T., Hynes, L.W., Ougham, H., Peng, J. *et al.* (2002) Gibberellin-mediated proteasome-dependent degradation of the barley DELLA protein SLN1 repressor. *Plant Cell*, **14**, 3191–3200.

Fuss, J., Liegmann, O., Krause, K. & Rensing, S.A. (2013) Green targeting predictor and ambiguous targeting predictor 2: the pitfalls of plant protein targeting prediction and of transient protein expression in heterologous systems. *The New Phytologist*, **200**, 1022–1033.

Glime, J.M. (2017) Ecophysiology of Development: Spore Germination. Online Book.

Graeber, K., Linkies, A., Steinbrecher, T., Mummenhoff, K., Tarkowska, D., Tureckova, V. *et al.* (2014) DELAY OF GERMINATION 1 mediates a conserved coat-dormancy mechanism for the temperature- and gibberellin-dependent control of seed germination. *Proceedings of the National Academy of Sciences of the United States of America*, **111**, E3571–E3580.

Graeber, K., Nakabayashi, K., Miatton, E., Leubner-Metzger, G. & Soppe, W.J. (2012) Molecular mechanisms of seed dormancy. *Plant, Cell & Environment*, **35**, 1769–1786.

Gremer, J.R., Kimball, S. & Venable, D.L. (2016) Within-and among-year germination in Sonoran Desert winter annuals: bet hedging and predictive germination in a variable environment. *Ecology Letters*, **19**, 1209–1218.

Harrison, C.J., Roeder, A.H., Meyerowitz, E.M. & Langdale, J.A. (2009) Local cues and asymmetric cell divisions underpin body plan transitions in the moss *Physcomitrella patens*. *Current Biology*, **19**, 461–471.

Hirano, K., Asano, K., Tsuji, H., Kawamura, M., Mori, H., Kitano, H. *et al.* (2010) Characterization of the molecular mechanism underlying gibberellin perception complex formation in rice. *Plant Cell*, **22**, 2680–2696.

Hiss, M., Meyberg, R., Westermann, J., Haas, F.B., Schneider, L., Schallenberg-Rudinger, M. *et al.* (2017) Sexual reproduction, sporophyte development and molecular variation in the model moss *Physcomitrella patens*: introducing the ecotype Reute. *The Plant Journal*, **90**, 606–620.

Hiss, M., **Schneider, L.**, **Grosche, C.**, **Barth, M.A.**, **Neu, C.**, **Symeonidi, A.** ***et al.*** (2017) Combination of the endogenous lhcsr1 promoter and codon usage optimization boosts protein expression in the moss *Physcomitrella patens*. *Frontiers in Plant Science*, **8**, 1842.

Holdsworth, M.J., **Bentsink, L.** & **Soppe, W.J.J.** (2008) Molecular networks regulating Arabidopsis seed maturation, after-ripening, dormancy and germination. *The New Phytologist*, **179**, 33–54.

Huo, H., **Wei, S.** & **Bradford, K.J.** (2016) DELAY OF GERMINATION1 (DOG1) regulates both seed dormancy and flowering time through microRNA pathways. *Proceedings of the National Academy of Sciences of the United States of America*, **113**, E2199–E2206.

Ishikawa, M., **Murata, T.**, **Sato, Y.**, **Nishiyama, T.**, **Hiwatashi, Y.**, **Imai, A.** ***et al.*** (2011) Physcomitrella cyclin-dependent kinase a links cell cycle reactivation to other cellular changes during reprogramming of leaf cells. *Plant Cell*, **23**, 2924–2938.

Jernigan, K.K. & **Bordenstein, S.R.** (2014) Ankyrin domains across the tree of life. *PeerJ*, **2**, e264.

Katoh, K. & **Standley, D.M.** (2013) MAFFT multiple sequence alignment software version 7: improvements in performance and usability. *Molecular Biology and Evolution*, **30**, 772–780.

Kendall, S.L., **Hellwege, A.**, **Marriot, P.**, **Whalley, C.**, **Graham, I.A.** & **Penfield, S.** (2011) Induction of dormancy in Arabidopsis summer annuals requires parallel regulation of DOG1 and hormone metabolism by low temperature and CBF transcription factors. *Plant Cell*, **23**, 2568–2580.

Kenrick, P. (2017) How land plant life cycles first evolved. *Science*, **358**, 1538–1539.

King, K.E., **Moritz, T.** & **Harberd, N.P.** (2001) Gibberellins are not required for normal stem growth in Arabidopsis thaliana in the absence of GAI and RGA. *Genetics*, **159**, 767–776.

Knop, W. (1868) *Der Kreislauf des Stoffs: Lehrbuch der Agricultur-Chemie*. Leipzig: H. Haessel.

Labandera, A.M., **Tedds, H.M.**, **Bailey, M.**, **Sprigg, C.**, **Etherington, R.D.**, **Akintewe, O.** ***et al.*** (2021) The PRT6 N-degron pathway restricts VERNALIZATION 2 to endogenous hypoxic niches to modulate plant development. *The New Phytologist*, **229**, 126–139.

Lang, D., **Ullrich, K.K.**, **Murat, F.**, **Fuchs, J.**, **Jenkins, J.**, **Haas, F.B.** ***et al.*** (2018) The *Physcomitrella patens* chromosome-scale assembly reveals moss genome structure and evolution. *The Plant Journal*, **93**, 515–533.

Lantzouni, O., **Alkofer, A.**, **Falter-Braun, P.** & **Schwechheimer, C.** (2020) GROWTH-REGULATING FACTORS interact with DELLAs and regulate growth in cold stress. *Plant Cell*, **32**, 1018–1034.

Larkin, M.A., **Blackshields, G.**, **Brown, N.P.**, **Chenna, R.**, **McGettigan, P.A.**, **McWilliam, H.** ***et al.*** (2007) Clustal W and Clustal X version 2.0. *Bioinformatics*, **23**, 2947–2948.

Lee, S., **Cheng, H.**, **King, K.E.**, **Wang, W.**, **He, Y.**, **Hussain, A.** ***et al.*** (2002) Gibberellin regulates Arabidopsis seed germination via RGL2, a GAI/RGA-like gene whose expression is up-regulated following imbibition. *Genes & Development*, **16**, 646–658.

Lim, S., **Park, J.**, **Lee, N.**, **Jeong, J.**, **Toh, S.**, **Watanabe, A.** ***et al.*** (2013) ABA-insensitive3, ABA-insensitive5, and DELLAs interact to activate the expression of SOMNUS and other high-temperature-inducible genes in imbibed seeds in Arabidopsis. *Plant Cell*, **25**, 4863–4878.

Liu, X. & **Hou, X.** (2018) Antagonistic regulation of ABA and GA in metabolism and signaling pathways. *Frontiers in Plant Science*, **9**, 251.

Marin-de la Rosa, N., **Sotillo, B.**, **Miskolczi, P.**, **Gibbs, D.J.**, **Vicente, J.**, **Carbonero, P.** ***et al.*** (2014) Large-scale identification of gibberellin-related transcription factors defines group VII ETHYLENE RESPONSE FACTORS as functional DELLA partners. *Plant Physiology*, **166**, 1022–1032.

Menand, B., **Calder, G.** & **Dolan, L.** (2007) Both chloronemal and caulonemal cells expand by tip growth in the moss *Physcomitrella patens*. *Journal of Experimental Botany*, **58**, 1843–1849.

Merai, Z., **Graeber, K.**, **Wilhelmsson, P.**, **Ullrich, K.K.**, **Arshad, W.**, **Grosche, C.** ***et al.*** (2019) Aethionema arabicum: a novel model plant to study the light control of seed germination. *Journal of Experimental Botany*, **70**, 3313–3328.

Milne, I., **Stephen, G.**, **Bayer, M.**, **Cock, P.J.**, **Pritchard, L.**, **Cardle, L.** ***et al.*** (2013) Using tablet for visual exploration of second-generation sequencing data. *Briefings in Bioinformatics*, **14**, 193–202.

Miyazaki, S., **Hara, M.**, **Ito, S.**, **Tanaka, K.**, **Asami, T.**, **Hayashi, K.I.** ***et al.*** (2018) an ancestral gibberellin in a moss *Physcomitrella patens*. *Molecular Plant*, **11**, 1097–1100.

Moody, L.A., **Saidi, Y.**, **Gibbs, D.J.**, **Choudhary, A.**, **Holloway, D.**, **Vesty, E.F.** ***et al.*** (2016) An ancient and conserved function for armadillo-related proteins in the control of spore and seed germination by abscisic acid. *The New Phytologist*, **211**, 940–951.

Moore, A.D., **Held, A.**, **Terrapon, N.**, **Weiner, J.**, **3rd** & **Bornberg-Bauer, E.** (2014) DoMosaics: software for domain arrangement visualization and domain-centric analysis of proteins. *Bioinformatics*, **30**, 282–283.

Mosavi, L.K., **Cammett, T.J.**, **Desrosiers, D.C.** & **Peng, Z.Y.** (2004) The ankyrin repeat as molecular architecture for protein recognition. *Protein Science*, **13**, 1435–1448.

Murase, K., **Hirano, Y.**, **Sun, T.P.** & **Hakoshima, T.** (2008) Gibberellin-induced DELLA recognition by the gibberellin receptor GID1. *Nature*, **456**, 459–463.

Nakabayashi, K., **Bartsch, M.**, **Xiang, Y.**, **Miatton, E.**, **Pellengahr, S.**, **Yano, R.** ***et al.*** (2012) The time required for dormancy release in Arabidopsis is determined by DELAY OF GERMINATION1 protein levels in freshly harvested seeds. *Plant Cell*, **24**, 2826–2838.

Nee, G., **Kramer, K.**, **Nakabayashi, K.**, **Yuan, B.**, **Xiang, Y.**, **Miatton, E.** ***et al.*** (2017) DELAY OF GERMINATION1 requires PP2C phosphatases of the ABA signalling pathway to control seed dormancy. *Nature Communications*, **8**, 72.

Nishimura, N., **Tsuchiya, W.**, **Moresco, J.J.**, **Hayashi, Y.**, **Satoh, K.**, **Kaiwa, N.** ***et al.*** (2018) Control of seed dormancy and germination by DOG1-AHG1 PP2C phosphatase complex via binding to heme. *Nature Communications*, **9**, 2132.

Nishiyama, E., **Nonogaki, M.**, **Yamazaki, S.**, **Nonogaki, H.** & **Ohshima, K.** (2021) Ancient and recent gene duplications as evolutionary drivers of the seed maturation regulators DELAY OF GERMINATION1 family genes. *The New Phytologist*, **230**, 889–901.

Nonogaki, M., **Yamazaki, S.**, **Nishiyama, E.**, **Ohshima, K.** & **Nonogaki, H.** (2022) Seed traits and phylogenomics: prospects for the 21st century. *Seed Science Research*, **32**, 137–143.

Park, J., **Nguyen, K.T.**, **Park, E.**, **Jeon, J.S.** & **Choi, G.** (2013) DELLA proteins and their interacting RING finger proteins repress gibberellin responses by binding to the promoters of a subset of gibberellin-responsive genes in Arabidopsis. *Plant Cell*, **25**, 927–943.

Perroud, P.F., **Haas, F.B.**, **Hiss, M.**, **Ullrich, K.K.**, **Alboresi, A.**, **Amirebrahimi, M.** ***et al.*** (2018) The *Physcomitrella patens* gene atlas project: large-scale RNA-seq based expression data. *The Plant Journal*, **95**, 168–182.

Phokas, A. & **Coates, J.C.** (2021) Evolution of DELLA function and signaling in land plants. *Evolution & Development*, **23**, 137–154.

Phokas, A., **Meyberg, R.**, **Briones-Moreno, A.**, **Hernandez-Garcia, J.**, **Wadsworth, P.T.**, **Vesty, E.F.** ***et al.*** (2023) DELLA proteins regulate spore germination and reproductive development in *Physcomitrium patens*. *The New Phytologist*, **238**, 654–672.

Puttick, M.N., **Morris, J.L.**, **Williams, T.A.**, **Cox, C.J.**, **Edwards, D.**, **Kenrick, P.** ***et al.*** (2018) The interrelationships of land plants and the nature of the ancestral embryophyte. *Current Biology*, **28**, 733–745.e732.

Rensing, S.A. (2016) (Why) Does Evolution Favour Embryogenesis? *Trends in Plant Science*, **21**, 562–573.

Rensing, S.A., **Goffinet, B.**, **Meyberg, R.**, **Wu, S.Z.** & **Bezanilla, M.** (2020) The moss physcomitrium (*Physcomitrella*) patens: a model organism for non-seed plants. *Plant Cell*, **32**, 1361–1376.

Rombola-Caldentey, B., **Rueda-Romero, P.**, **Iglesias-Fernandez, R.**, **Carbonero, P.** & **Onate-Sanchez, L.** (2014) Arabidopsis DELLA and two HD-ZIP transcription factors regulate GA signaling in the epidermis through the L1 box cis-element. *Plant Cell*, **26**, 2905–2919.

Ronquist, F., **Teslenko, M.**, **van der Mark, P.**, **Ayres, D.L.**, **Darling, A.**, **Hohna, S.** ***et al.*** (2012) MrBayes 3.2: efficient Bayesian phylogenetic inference and model choice across a large model space. *Systematic Biology*, **61**, 539–542.

Sall, K., **Dekkers, B.J.W.**, **Nonogaki, M.**, **Katsuragawa, Y.**, **Koyari, R.**, **Hendrix, D.** ***et al.*** (2019) DELAY OF GERMINATION 1-LIKE 4 acts as an inducer of seed reserve accumulation. *The Plant Journal*, **100**, 7–19.

Sasaki, A., **Itoh, H.**, **Gomi, K.**, **Ueguchi-Tanaka, M.**, **Ishiyama, K.**, **Kobayashi, M.** ***et al.*** (2003) Accumulation of phosphorylated repressor for gibberellin signaling in an F-box mutant. *Science*, **299**, 1896–1898.

Schaefer, D.G., **Delacote, F.**, **Charlot, F.**, **Vrielynck, N.**, **Guyon-Debast, A.**, **Le Guin, S.** ***et al.*** (2010) RAD51 loss of function abolishes gene targeting and de-represses illegitimate integration in the moss *Physcomitrella patens*. *DNA Repair (Amst)*, **9**, 526–533.

Sedgwick, S.G. & **Smerdon, S.J.** (1999) The ankyrin repeat: a diversity of interactions on a common structural framework. *Trends in Biochemical Sciences*, **24**, 311–316.

Shu, K., **Zhou, W.**, **Chen, F.**, **Luo, X.** & **Yang, W.** (2018) Abscisic acid and gibberellins antagonistically mediate plant development and abiotic stress responses. *Frontiers in Plant Science*, **9**, 416.

Tyler, L., **Thomas, S.G.**, **Hu, J.**, **Dill, A.**, **Alonso, J.M.**, **Ecker, J.R.** ***et al.*** (2004) Della proteins and gibberellin-regulated seed germination and floral development in Arabidopsis. *Plant Physiology*, **135**, 1008–1019.

Ueguchi-Tanaka, M., **Ashikari, M.**, **Nakajima, M.**, **Itoh, H.**, **Katoh, E.**, **Kobayashi, M.** ***et al.*** (2005) GIBBERELLIN INSENSITIVE DWARF1 encodes a soluble receptor for gibberellin. *Nature*, **437**, 693–698.

Vesty, E.F., **Saidi, Y.**, **Moody, L.A.**, **Holloway, D.**, **Whitbread, A.**, **Needs, S.** ***et al.*** (2016) The decision to germinate is regulated by divergent molecular networks in spores and seeds. *The New Phytologist*, **211**, 952–966.

Waterhouse, A.M., **Procter, J.B.**, **Martin, D.M.**, **Clamp, M.** & **Barton, G.J.** (2009) Jalview version 2—a multiple sequence alignment editor and analysis workbench. *Bioinformatics*, **25**, 1189–1191.

Xi, W., **Liu, C.**, **Hou, X.** & **Yu, H.** (2010) MOTHER OF FT AND TFL1 regulates seed germination through a negative feedback loop modulating ABA signaling in Arabidopsis. *Plant Cell*, **22**, 1733–1748.

Yasumura, Y., **Crumpton-Taylor, M.**, **Fuentes, S.** & **Harberd, N.P.** (2007) Step-by-step acquisition of the gibberellin-DELLA growth-regulatory mechanism during land-plant evolution. *Current Biology*, **17**, 1225–1230.

Yoshida, H., **Hirano, K.**, **Sato, T.**, **Mitsuda, N.**, **Nomoto, M.**, **Maeo, K.** ***et al.*** (2014) DELLA protein functions as a transcriptional activator through the DNA binding of the indeterminate domain family proteins. *Proceedings of the National Academy of Sciences of the United States of America*, **111**, 7861–7866.